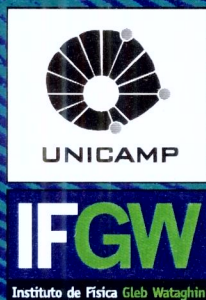


Abstracta

Ano IV - N.04



Agosto.02

Trabalhos Aceitos para Publicação em Periódicos.

A 018 - 02 Different Gd³⁺ sites in doped CaB₆: an electron spin resonance study.

A 019- 02 Field distribution and flux-line depinning in MgB₂

A 020 - 02 Short range interactions in a two-electron system: energy levels and magnetic properties.

Trabalhos Aceitos para Publicação em Conferências.

C 004 - 02 Ambipolar Diffusion and Spatial-and Time-Resolved Optical Spectroscopy in Semiconductor Heterostructures.

C 005 - 02 HOLOGRAFIA TELEVIDO.

TRABALHOS PUBLICADOS JULHO/AGOSTO 2002

P 058 -02 à P 085-02.

Trabalhos aceitos para publicação em Periódicos

A 018 - 02 Different Gd³⁺ sites in doped CaB₆: an electron spin resonance study.

R.R. Urbano,¹ C. Rettori,¹ G.E. Barberis,¹ M. Torelli,² A. Bianchi,² Z. Fisk,² P.G. Pagliuso,³ A. Malinowski,³ M.F. Hundley,³ J.L. Sarrao³ and S.B. Oseroff⁴

The local environment of Gd³⁺ (4f⁷, S=7/2) ions in single crystals of Ca_{1-x}Gd_xB₆ (0.0001 ≤ x ≤ 0.01) is studied by means of Electron Spin Resonance (ESR). The spectra for low concentration samples (x ≤ 0.001) show a split spectrum due to cubic crystal field effects (CFE). The lineshape of each fine structure line is lorentzian, indicating an insulating environment for the Gd³⁺ ions. For higher concentrations (0.003 ≤ x ≤ 0.01), the spectra show a single resonance (g=1.992(4), DH_{1/2} ~ 20-60 Oe) with no CFE and dysonian lineshape indicating metallic environment for the Gd³⁺ ions. For intermediate concentrations, a coexistence of spectra corresponding to insulating and metallic regions is observed. Most of the measured samples show the weak ferromagnetism (WF) as reported for Ca_{0.995}La_{0.005}B₆, but, surprisingly, this WF has no effect in our ESR spectra either for metallic or insulating environments. This result suggests that the WF in these systems might be isolated in clusters (defect-rich regions) and its relationship with metallicity is nontrivial.

Phys. Rev. B. 65, 180407 (2002).

A 019-02 Field distribution and flux-line depinning in MgB₂

R.R. Urbano¹, P.G. Pagliuso¹, C. Rettori¹, Y. Kopelevich¹, N.O. Moreno², and J.L. Sarrao²

We report the first observation of the field distribution and flux-line lattice (FLL) depinning in the vortex-state (VS) of a type-II superconductor probed by conduction electrons spin resonance (CESR). CESR was performed in MgB₂ (T ~ 39 K) at 4.1 GHz (1455 Oe) and 9.5 GHz (3390 Oe). The field distribution, n(H), and a standard deviation of s ~ 14 Oe (at 28 K/4.1 GHz and at 7 K/9.5 GHz) were inferred, respectively, from the distortion and broadening of the CESR in the VS. For both frequencies the FLL depinning temperature was determined.

Phys. Rev. Lett. 89(8), 087602 (2002).

A 020 - 02 Short range interactions in a two-electron system: energy levels and magnetic properties.

L.G.G.V. Dias da Silva and M.A.M. de Aguiar

The problem of two electrons in a square billiard interacting via a finite-range repulsive Yukawa potential and subjected to a constant magnetic field is considered. We compute the energy spectrum for both singlet and triplet states, and for all symmetry classes, as a function of the strength and range of the interaction and of the magnetic field. We show that the short-range nature of the potential suppresses the formation of "Wigner molecule" states for the ground state, even in the strong interaction limit. The magnetic susceptibility χ(B) shows low-temperature paramagnetic peaks due to exchange induced singlet-triplet oscillations. The position, number and intensity of these peaks depend on the range and strength of the interaction. The contribution of the interaction to the susceptibility displays paramagnetic and diamagnetic phases as a function of T.

Physical Review B, accepted on august 2002.

Trabalhos Aceitos para Publicação em Conferências.

C 004 - 02 Ambipolar Diffusion and Spatial-and Time-Resolved Optical Spectroscopy in Semiconductor Heterostructures.

Áurea R. Vasconcellos, M. J. Brasil, Javier Alvarado, Marcus V. Mesquita, Roberto Luzzi.

Proceedings of the 2002- international Conference on the Physics of Semiconductors; Edinburgh, Escocia, 2002.

C 005 - 02 HOLOGRAFIA TELEVIDO.

Lunazzi, J. J.

La fizikaj principoj kaj rezultoj de la holografia tekniko, perfektaj tridimensiaj bildoj, revigis la homaron pri holografia televido. Pluraj sistemoj ekzistas por montri tridimensiajn movbildojn sen la uzo de specialaj okulvitroj, sed nur kelkaj el ili montras la bildojn shanghante laŭ la vidpunkto (paralakso). Se oni aldonas al tiu kondiĉo, ke la shangho laŭ vidpunkto okazu por pluraj spektantoj samtempe, restas nur du proponoj krom tiu bazita sur difrakta ekrano. Estas dezirinde plenumi ankaŭ la kondiĉojn:

- esti kaptebla per kamerao, samtempe al la okazajho.
- ne postuli troan kvanton da informo po bildo.
- funkcii per blanka lumo, ne per lasero.

La sistemo proponata de mi estas la nura, kiu enhavas chiujn tiujn kondiĉojn. Ghi estas bazita sur la kolekto aŭ registrado de paralelaj sinsekvaj tranĉoj de la sceno per vidkamerao. Unu ensemblo de tranĉoj kiuj atingas la tutan scenon faras unu volumenan bildon, kiun ni povas reprezenti al aro da observantoj per la uzado de difrakta kodigo de blanka lumo kaj difrakta (holografia) ekrano. La rapida shangho de volumenaj bildoj farighas volumena televido aŭ holografia televido. La metodo estis jam elprovita definitive dum la jaro 1998 per la farado de bildoj ne registritaj sed perkomputele desegnitaj kaj la provo por televido, eĉ se ankoraŭ ne farita, rezultas facile antaŭvidebla. La grando de la bildo atingas 500 litrojn (litro estas unuo, kiun mi konsilas apliki por mezuri tridimensiajn bildojn), per ekrano 0,85 m largha kaj 1,14 m alta, samtempe videbla de 6 homoj.

87a Universala Kongreso de Esperanto- Internacia Kongresa Universitato Fortaleza-CE-BR 3 a 10 de agosto de 2002 p.25-32

Trabalhos Publicados

P 058 - 02 "A joint Wigner function of an atom-field system with dissipation".

Sanz, L. and Furuya, K.

We found analytically the exact joint Wigner function (WF) of an atom-field system described by the Jaynes-Cummings model in the dispersive limit for a given initial state. Using the solution of a master equation with a dissipative term calculated by Peixoto de Faria and Nemes (Peixoto de Faria J G and Nemes M C 1999 *Phys. Rev. A* 59 3918) and a general expression for the joint WF proposed by Czirjak and Benedict (Czirjak A and Benedict M G 1996 *Quantum Semiclass. Opt.* 8 975), we obtained the exact reduced atom and field WFs and analysed their time evolution. Our results show that, at the maximum entanglement times, the atom tends to a statistical mixture state represented by a spherical polar plot. Also, the atomic WF shows how fast the negative-valued part disappears as a function of dissipation constant and the strength of the field coherent state.

Journal of Optics B-Quantum and Semiclassical Optics 4[3], S184-S190. 2002.

Trabalhos Publicados

P 059 - 02 "Antiparticles and light element isotope ions in the earth's magnetosphere".

Pugacheva, G. I., Gusev, A. A., Jayanthi, U., Martin, I. M., and Spjeldvik, W. N.

The ratio of positron/electron fluxes originating in nuclear reactions in the Earth's Magnetosphere is considered. It is supposed that positrons as well as electrons are mainly produced in the decay of charged pions $\pi^{+/-} \rightarrow \mu^{+/-} \rightarrow e^{+/-}$ born in nuclear collisions of trapped relativistic inner zone protons and of cosmic rays with the residual atmosphere. These positrons and electrons are captured in the magnetosphere and create a positron and electron radiation belt of nuclear origin. The positron/electron trapped magnetospheric fluxes formed with this mechanism from radiation belt proton source are simulated and the resulting computed e^{+}/e^{-} flux ratio approximate to 4 appears to be in agreement with the recent observations made by the Alpha Magnetic Spectrometer (AMS) (The AMS collaboration, 1999). A > 200 MeV positron flux with an intensity about 4 times higher than the electron flux of the same energy was registered in the equatorial region at the attitude of 400 km. This ratio is significantly different from the computed ratio approximate to 1 obtained from the primary cosmic ray source through the same mechanism. As our modeling of nuclear spallation reaction shows, in the same reaction nuclei of isotopes of hydrogen and helium are also produced, which are the source of light element isotope radiation belts of D, T, He-3 and He-4 with a significant excess of He-3 over He-4 fluxes. The AMS instrument, as we have known, also looked at the distribution of helium nuclei and only He-3 was observed, which is one more evidence in favor of the above hypothesis. (C) 2002 Elsevier Science Ltd. All rights reserved.

Journal of Atmospheric and Solar-Terrestrial Physics 64[5-6], 625-631. 2002.

P 060 - 02 "Boron doping of hydrogenated amorphous silicon prepared by rf- co-sputtering".

de Lima, M. M., Freire, F. L., and Marques, F. C.

This paper addresses the doping mechanism of amorphous semiconductors through the investigation of boron doped rf co- sputtered amorphous hydrogenated silicon. The activation energy and room temperature conductivity varied from 0.9 to 0.3 eV and from $10^{(-12)}$ to $10^{(-4)}$ $\Omega^{-1} \cdot \text{cm}^{(-1)}$, respectively, by ranging the boron concentration from 0 to 3 at.%. These ranges of electronic properties are of the same order of those reported for samples prepared by plasma enhanced chemical vapor deposition (PECVD). In spite of these similarities, there are some relevant differences. The doping efficiency, at low boron concentrations, is much lower than that of PECVD samples. In addition, the creation of deep defects (dangling bonds) does not follow the square root power law dependence on the boron concentration as proposed by Street and observed in PECVD samples. These differences are associated with the density of defects, which is much higher in films prepared by sputtering. The increase in the deep defect density is more likely related to topological disorder, introduced by the presence of a high concentration of inactive impurities.

Brazilian Journal of Physics 32[2], 379-382. 2002.

P 061 - 02 "Carrier dynamics investigated by time resolved optical spectroscopy".

Luyo, S. J., Brasil, M. S. P., de Carvalho, H. B., de Carvalho, W., and Bernussi, A. A.

We have investigated the transport of carriers in GaAs using time resolved optical spectroscopy with picosecond resolution. Carriers are optically created to the sample surface by an ultra-fast laser pulse. They diffuse and drift through a thick GaAs layer, until they are captured by an InGaAs quantum well, where they recombine with holes from a p-type doped layer at an inner InGaP barrier. Our study was performed with a set of samples with different GaAs layer thickness. As the GaAs thickness increases, the emission from the quantum well is delayed and its decay slows down significantly. We have investigated the effect of an applied DC field between the surface and the InGaAs quantum well. The transient of the quantum well emission is mostly independent of the applied DC voltage up to field of the order of 20 KV/cm, including both polarities. This is a clear indication that the carrier transport is dominated by ambipolar diffusion due to the Coulomb interaction that strongly couples photoinjected electrons and holes. On the other hand, the decay of the GaAs emission varies significantly when a DC gate voltage is applied such as a current appears at the structure.

Brazilian Journal of Physics 32[2], 353-355. 2002.

P 062 - 02 "CERN to Gran Sasso; an ideal distance for superbeam?"

Minakata, H. and Nunokawa, H.

We use the CP trajectory diagram as a tool for pictorial representation of the genuine CP and the matter effects to explore the possibility of an in situ simultaneous measurement of δ and the sign of $\Delta m_{13}(2)$. We end up with a low- energy conventional superbeam experiment with a megaton-class water Cherenkov detector and baseline length of about 700 km. A picturesque description of the combined ambiguity which may arise in simultaneous determination of θ_{13} and the above two quantities is given in terms of CP trajectory diagram.

Nuclear Physics B-Proceedings Supplements 110, 404-406. 2002.

P 063 - 02 "Diffusive-like minibands in finite superlattices of disordered quantum wells".

Rey-Gonzalez, R. R., Machado, E., and Schulz, P. A.

The existence of quantized levels, as a consequence of spatial confinement, does not necessarily imply in formation of superlattices minibands due to the coupling between these quantum wells. The present work discuss a framework to analyze the analogue to minibands in periodic superlattices made of disordered quantum wells. The inter quantum well coupling leads to diffusive-like minibands.

Brazilian Journal of Physics 32[2], 341-343. 2002

P 064 - 02 "Effect of hydrogen and oxygen on stainless steel nitriding".

Figueroa, C. A., Wisnivesky, D., and Alvarez, F.

The influence of hydrogen and oxygen on stainless steel implanted by nitrogen low-energy ions is systematically studied. It is shown that hydrogen intervenes moderately in the process only when the oxygen partial pressure in the deposition chamber is relatively high. For very low-oxygen partial pressures, the energetic nitrogen molecules impinging on the substrate sputter the thin oxide layer formed on the substrate. This allows the growing of a rich nitrogen layer beneath the surface, improving the diffusing of the implanted atom deeper in the bulk material. For higher-oxygen partial pressures, the sputtering is ineffective, and an oxide layer partially covers the surface even in the presence of hydrogen. The maximum depth penetration of nitrogen depends on the degree of oxygen coverage, which is fairly well described by a Langmuir absorption isothermal. Hardness depth profiling is consistent with the existence of a diffusion barrier formed by the oxygen absorbed on the surface. In order to understand the role of hydrogen on the nitriding process, samples preimplanted with hydrogen were subsequently treated with nitrogen and the hardness depth profiling analyzed. These results may provide a clue about the practical consequences of oxygen and hydrogen on the nitriding process. (C) 2002 American Institute of Physics.

Journal of Applied Physics 92[2], 764-770. 2002.

P 065 - 02 "Effect of the lead dimensionality over transport properties in quantum dots".

Craco, L. and Cuniberti, G.

We theoretically investigate the effect of the lead dimensionality on the non-equilibrium electron transport through quantum dots. More precisely, we study nonlinear transport in a quantum dot coupled to leads of diverse dimensionality. We show that the presence of the latter strongly determines the resulting transport properties. Differently from higher dimensional leads (wide and smooth band limit), van Hove singularities in the density of states of low-dimensional reservoirs determine sharp resonances in the differential conductance at finite applied voltages as well as in the dot spectral density. It is also shown that, due to the finiteness of the terminal bandwidth, the differential conductance change its sign at higher biases. These results clearly indicate that the environment does play an important role in determining transport properties in mesoscopic systems.

Brazilian Journal of Physics 32[2], 293-295. 2002.

P 066 - 02 "Elastic and absorption cross sections for electron-nitrous oxide collisions".

Lee, M. T., Iga, I., Homem, M. G. P., Machado, L. E., and Brescansin, L. M.

In this work, we present a joint theoretical-experimental study on electron-N₂O collisions in the intermediate energy range. More specifically, calculated and measured elastic differential, integral, and momentum-transfer cross sections, as well as calculated total and absorption cross sections are reported. The measurements were performed using a crossed electron-beam-molecular-beam geometry. The angular distribution of the scattered electrons was converted to absolute cross sections using the relative-flow technique. Theoretically, a complex optical potential is used to represent the electron-molecule interaction dynamics in the present calculation. The Schwinger variational iterative method combined with the distorted-wave approximation is used to solve the scattering equations. The comparison of the present calculated results with the measured results as well as with the existing experimental and theoretical data shows good agreement.

Physical Review A 65[6], art-062702. 2002.

P 067 - 02 "Electron mobility in nitride materials".

Rodrigues, C. G., Freire, V. N., Vasconcellos, A. R., and Luzzi, R.

We contribute here a theoretical study of the electron mobility in n-doped GaN, InN, and AlN at moderate to high electric fields. We solve the set of coupled nonlinear integro-differential equations of evolution to obtain the steady-state values of the basic intensive nonequilibrium thermodynamic variables for the three materials. The regions with ohmic and non-ohmic behavior in the electron drift velocity dependence on the electric field strength axe characterized in the three nitrides. The electron mobility is calculated, and it is shown that the larger corresponds to InN, and the smaller to AlN.

Brazilian Journal of Physics 32[2], 439-441. 2002.

P 068 - 02 "ESR observations of paramagnetic centers in intrinsic hydrogenated microcrystalline silicon".

de Lima, M. M., Taylor, P. C., Morrison, S., LeGeune, A., and Marques, F. C.

Paramagnetic centers in hydrogenated microcrystalline silicon, $\mu\text{-Si:H}$ have been studied using dark and light-induced electron-spin resonance (ESR). In dark ESR measurements only one center is observed. The g values obtained empirically from powder-pattern line-shape simulations are $g(\text{parallel to})=2.0096$ and $g(\text{perpendicular to})=2.0031$. We suggest that this center may be due to defects in the crystalline phase. During illumination at low temperatures, an additional ESR signal appears. This signal is best described by two powder patterns indicating the presence of two centers. One center is asymmetric ($g(\text{parallel to})=1.999$, $g(\text{perpendicular to})=1.996$), while the other is characterized by large, unresolved broadening such that unique g values cannot be obtained. The average g value for this center is 1.998. The light-induced signal, which we interpret as coming from carriers trapped in the band tails at the crystalline grain boundaries, remains for at least several minutes after the light is turned off. Although the time scales of the decay curves are very different for two samples prepared by different techniques, both decays can be fitted using the assumption of recombination due to distant pairs of electrons and holes trapped in localized band-tail states.

Physical Review B 65[23], art-235324. 2002.

P 069 - 02 "Future tests of non-standard neutrino interactions".

Gago, A. M., Guzzo, M. M., Nunokawa, H., Teves, W. J. C., and Funchal, R. Z.

We explore non-standard neutrino matter interactions, working as sub-leading effects in the standard mass oscillation framework. Both mechanisms working together, induce a magnifying fake CP violating effect in the presence of matter, which can be studied in a neutrino factory which is based on a muon storage ring. Considering the three neutrino scheme, assuming a 10 kt detector with 5 years of operation, a stored muon energy E_μ greater than or equal to 20 GeV, 2×10^{20} muon decays per year, and a baseline L similar to 732 km, we show that it is possible to test non-standard flavor changing neutrino interactions down to the level of $(10^{-3} - 10^{-2}) G(F)$, in both $\nu_\mu \rightarrow \nu(r) / \langle \nu \rangle_{\text{bar}}$ ($\mu \rightarrow \langle \nu \rangle_{\text{bar}}$) and $\nu(e) \rightarrow \nu(r) / \langle \nu \rangle_{\text{bar}}$ ($e \rightarrow \langle \nu \rangle_{\text{bar}}$) modes.

Nuclear Physics B-Proceedings Supplements 110, 407-409. 2002.

P 070 - 02 "Giant magnetoimpedance: concepts and recent progress".

Knobel, M. and Pirota, K. R.

The giant magnetoimpedance effect (GMI) consists in drastic changes of the complex impedance of soft magnetic materials upon the application of an external magnetic field. The GMI effect is strongly dependent on the frequency of the applied current and the magnetic anisotropies present in the material, among other factors, which spawn a number of interesting new magnetic phenomena. In this context, one can roughly separate the research on GMI into approximately three aspects: (i) theory; (ii) applications and (iii) as a tool to investigate other magnetic parameters. In this work, an updated review of all these aspects is given. (C) 2002 Elsevier Science B.V. All rights reserved.

Journal of Magnetism and Magnetic Materials 242, 33-40. 2002.

P 071 - 02 "Laser effects in semiconductor heterostructures within an extended dressed-atom approach".

Brandi, H. S., Latge, A., and Oliveira, L. E.

We extend the dressed-atom approach to treat the interaction of a laser field with a semiconductor system. The semiconductor is modeled via a simple Kane band-structure scheme and the interaction with the laser field is incorporated through the renormalization of the semiconductor energy gap and conduction/valence effective masses. Far from resonances, such one-body approach allows the study of the effects of laser fields on a variety of optoelectronic phenomena in semiconductor systems for which the effective-mass approximation provides a good physical description. We calculate the effects originated by the laser-dressing on the donor and exciton peak energies in quantum-well heterostructures, and show that they may be quite considerable and observable.

Brazilian Journal of Physics 32[2], 262-265. 2002.

P 072 - 02 "LMA parameters and non-zero Ue_3 effects oil atmospheric nu data?"

Peres, O. L. G. and Smirnov, A. Y.

We study the possible manifestation of the interference between the effects produced in the atmospheric neutrinos due to oscillation driven by the solar parameters parameters Δm_{21}^2 and $\sin^2 2\theta_{12}$ and due to oscillation driven by Δm_{31}^2 and Ue_3 .

Nuclear Physics B-Proceedings Supplements 110, 355-357. 2002.

P 073 - 02 "Local order of Sb and Bi dopants in hydrogenated amorphous germanium thin films studied by extended x-ray absorption fine structure".

Dalba, G., Fornasini, P., Grisenti, R., Rocca, F., and Chambouleyron, I.

This letter reports on the investigation of the local order and coordination of Sb and Bi impurities in hydrogenated amorphous germanium thin films. The study uses the extended x-ray absorption fine structure technique in fluorescence mode at room temperature. The investigation includes doping concentrations ranging from 1.1×10^{19} to 5×10^{20} cm⁻³. For both impurities, the evidence is that the thermal equilibrium model is not applicable in this case. This result qualitatively follows the behavior of Ga and In impurities in hydrogenated amorphous germanium (a-Ge:H) samples except for Bi. These findings are consistent with data on the transport properties of Sb- and Bi-doped a-Ge:H films. (C) 2002 American Institute of Physics.

Applied Physics Letters 81[4], 625-627. 2002.

P 074 - 02 "Magnetic properties of gadolinium-doped amorphous silicon films".

Sercheli, M. S., Rettori, C., and Zanatta, A. R.

Electron spin resonance (ESR) and dc-magnetization experiments have been performed in Gd-doped amorphous (a-)silicon films. The films were deposited by the cosputtering technique following different conditions rendering samples

with varying Gd and hydrogen concentrations. In addition to films with different contents of impurities and, in order to probe the influence of the atomic structure on the magnetic properties of the Gd species, the films were also submitted to laser-induced crystallization processing. Both ESR and dc-magnetization results show that Gd is incorporated as a trivalent ion (Gd³⁺) in the Si host. ESR data indicate a strong dependence between the Gd concentration and the density of Si dangling bonds. Moreover, the Gd³⁺ local environment is nearly insensitive to the Gd and H content, as well as to the atomic structure of the Si host. Along with gadolinium, other rare-earth species have been investigated and the main results are discussed.

Brazilian Journal of Physics 32[2], 409-411. 2002.

P 075 - 02 "Magnetoabsorption spectra of intraexcitonic transitions in GaAs-(Ga,Al)As semiconductor quantum wells".

Barticevic, Z., Pacheco, M., Duque, C. A., and Oliveira, L. E.

We present a theoretical study, within the effective-mass approximation, of the magnetoabsorption spectra of intraexcitonic terahertz transitions of light-hole and heavy-hole confined magnetoexcitons in GaAs-(Ga,Al)As quantum wells. The semiconductor quantum wells are studied under magnetic fields applied in the growth direction of the semiconductor heterostructure. The various magnetoexciton states are obtained in the effective-mass approximation by an expansion of the exciton-envelope wave functions in terms of products of hole and electron quantum-well states with appropriate Gaussian functions for the various excitonic states. Intramagnetoexciton transitions are theoretically studied by exciting the allowed excitonic transitions with $\sigma(+)$ (or $\sigma(-)$) far-infrared radiation circularly polarized in the plane of the GaAs-(Ga,Al)As quantum well. Theoretical results are obtained for the intramagnetoexciton transition energies and magnetoabsorption spectra associated with excitations from 1s-like to 2p(+/-), and 3p(+/-)-like magnetoexciton states, and found in overall agreement with optically detected resonance measurements.

Journal of Applied Physics 92[3], 1227-1231. 2002.

P 076 - 02 "Metal nanowires: atomic arrangement and electrical transport properties".

Rodrigues, V. and Ugarte, D.

We have studied the atomic arrangement, and defect formation in metal nanowires (NWs) generated by mechanical elongation using in situ high resolution transmission electron microscopy. It has been observed that the narrowest constriction of gold and platinum NWs is crystalline and defect-free; in particular, gold NWs adopt only three kinds of atomic arrangement. A model correlating these gold structures and the quantum conductance behaviour is proposed, which showed a remarkable agreement with ultrahigh-vacuum mechanically controllable break junction electrical transport measurements.

Nanotechnology 13[3], 404-408. 2002.

P 077 - 02 "Optical studies of the correlation between interface disorder and the photoluminescence line shape in GaAs/InGaP quantum wells".

Laureto, E., Meneses, E. A., Carvalho, W., Bernussi, A. A., Ribeiro, E., da Silva, E. C. F., and de Oliveira, J. B. B.

Photoluminescence (PL) and excitation PL measurements have been performed at different temperatures in a number of lattice-matched GaAs/In_{0.49}Ga_{0.51}P quantum wells, where the fluctuations of the potential energy are comparable with the thermal energy of the photocreated carriers. Two samples with different well widths allow to observe a series of anomalous effects in their optical response. The observed effects are related to the disorder in the interface, characterizing fluctuations in the confinement potential energy. It is proposed that the carrier relaxation processes occur either at the local minima or at the absolute minimum of the confinement potential, depending on the ratio of the thermal energy and the magnitude of the potential fluctuations.

Brazilian Journal of Physics 32[2], 314-317. 2002.

P 078 - 02 "Phase-locking of superimposed diffractive gratings in photoresists".

Freschi, A. A., dos Santos, F. J., Rigon, E. L., and Cascato, L.

The superposition of optical interference patterns in a photoresist film can produce a rich variety of diffractive structures. In particular, a periodic non-sinusoidal surface relief profile can be synthesized by adding the Fourier components (sinusoidal gratings) of the desired profile. In order to control the shape of the grooves it is very important an accurate adjustment of the relative spatial shift between the recorded sinusoidal components. We describe the implementation of an opto-electronic feedback loop to select and lock such spatial shift at any desired position, thus allowing the synthesis of structures varying from symmetrical to asymmetrical relief profiles in a continuous range. To demonstrate the feasibility of the technique, the Fourier synthesis of two spatial harmonics is accomplished. The superposed sinusoidal gratings were recorded in positive photoresist films using a holographic setup operating at the line $\lambda = 457.9$ nm of an argon-ion laser. A detailed description of the procedure as well as the resulting profiles recorded in the photoresist is presented. (C) 2002 Elsevier Science B.V. All rights reserved.

Optics Communications 208[1-3], 41-49. 2002.

P 079 - 02 "Pulsed laser crystallization of SiGe alloys on GaAs".

Dondeo, F., Santos, P. V., Ramsteiner, M., Comedi, D., Pudenzi, M. A. A., and Chambouleyron, I.

We have investigated the crystallization of amorphous SiGe films deposited on crystalline GaAs (001) substrates using ns laser pulses. Analysis of the film structure using Raman spectroscopy indicates the formation of heteroepitaxial $\text{SixGe}_{1-x}/\text{GaAs}$ structures for Si compositions up to $x = 25\%$. Higher compositions lead to polycrystalline films. This is attributed to the increased lattice mismatch between SixGe_{1-x} and GaAs as the Si fraction in the alloy increases.

Brazilian Journal of Physics 32[2], 376-378. 2002.

P 080 - 02 "Spontaneous pattern formation and genetic invasion in locally mating and competing populations".

Sayama, H., de Aguiar, M. A. M., Bar-Yam, Y., and Baranger, M.

We present a theoretical model of evolution of spatially distributed populations in which organisms mate with and compete against each other only locally. We show using both analysis and numerical simulation that the typical dynamics of population density variation is a spontaneous formation of isolated groups due to competition for resources. The resulting spatial separation between groups strongly affects the process of genetic invasion by local reproductive mixing, and spatially inhomogeneous genetic distributions are possible in the final states. We then consider a specific version of this model in the presence of disruptive selection, favoring two fittest types against their genetic intermediates. This case can be simplified to a system that involves just two nonconserved order parameters: population density and type difference. Since the coexistence of two fittest types is unstable in this case, symmetry breaking and coarsening occur in type difference, implying eventual dominance by one type over another for finite populations. However, such coarsening patterns may be pinned by the spontaneously generated

spatial separation between isolated groups. The long-term evolution of genetic composition is found to be sensitive to the ratio of the mating and competition ranges, and other parameters. Our model may provide a theoretical basis for consideration of various properties of spatially extended evolutionary processes, including spontaneous formation of subpopulations and lateral invasion of different types.

Physical Review e 65[5], art-051919. 2002.P 081 - 02

P 081 -02 "Study of magnetic and specific heat measurements at low temperatures in $\text{Nd}_{0.5}\text{Sr}_{0.5}\text{MnO}_3$, $\text{Nd}_{0.5}\text{Ca}_{0.5}\text{MnO}_3$ ".

Lopez, J., Lisboa, P. N., de Lima, O. F., and Araujo-Moreira, F. M.

The magnetization at low temperatures for $\text{Nd}_{0.5}\text{Sr}_{0.5}\text{MnO}_3$ and $\text{Nd}_{0.5}\text{Ca}_{0.5}\text{MnO}_3$ samples showed a rapid increase with decreasing temperatures, contrary to a $\text{La}_{0.5}\text{Ca}_{0.5}\text{MnO}_3$ sample. Specific heat measurement at low temperatures showed a Schottky-like anomaly for the first two samples. However, there is no a straight forward correlation between the intrinsic magnetic moment of the Nd^{3+} ions and the Schottky-like anomaly.

Journal of Magnetism and Magnetic Materials 242, 683-685. 2002.

P 082 - 02 "Temperature dependence of hysteresis loops and AC- susceptibility of as-cast and annealed $\text{Nd}_{60}\text{Fe}_{30}\text{Al}_{10}$ hard magnetic alloy".

Triyono, D., Turtelli, R. S., Grossinger, R., Michor, H., Pirota, K. R., Knobel, M., Sassik, H., Mathias, T., Hofinger, S., and Fidler, J.

Magnetic properties of melt-spun $\text{Nd}_{60}\text{Fe}_{30}\text{Al}_{10}$ alloy were studied between 2 and 350K. The behaviour of the temperature dependence of coercive field is explained by the presence of magnetic multi-phases, which were determined by means of transmission electron microscopy and X-ray diffraction. Low coercivity at room temperature is attributed to the low Curie temperature of the amorphous phase. (C) 2002 Elsevier Science B.V. All rights reserved.

Journal of Magnetism and Magnetic Materials 242, 1321-1324. 2002.

P 083 - 02 "The role of oxygen partial pressure and annealing temperature on the formation of W=O bonds in thin WO_3 films".

Bittencourt, C., Landers, R., Llobet, E., Correig, X., and Calderer, J.

Thin films of tungsten oxide were deposited onto silicon substrates using reactive rf sputtering. The structure of the films is strongly dependent on the conditions of deposition and post-treatment. Important issues are the influences of oxygen pressure during deposition and of annealing temperature. We used x-ray photoelectron spectroscopy to investigate the in-depth composition of the films. The most surface sensitive O 1s core level spectra are made up of two structures, one generated by photoelectrons emitted from oxygen atoms in WO_3 (O-W-O) and other at lower energy generated by the photoelectrons emitted from oxygen atoms located at the boundary of the grains (W=O). Using Raman spectroscopy, an increase of the W=O/O-W-O ratio was correlated to an increase in the oxygen partial pressure

used during the deposition. A decrease of this ratio was observed while annealing temperature was increased, which was correlated to an increase in the size of the grains that form the films.
Semiconductor Science and Technology 17[6], 522-525. 2002.

P 084 - 02 "The Schwinger multichannel method (SMC) calculations for $Z(\text{eff})$ were off by a factor of Z ".

Varella, M. T. D., de Carvalho, C. R. C., and Lima, M. A. P.

Our previously reported $Z(\text{eff})$ values were in accidental agreement with experiment. They were actually underestimated by a factor of Z . In order to full understand the nature of the discrepancies with experimental data, we carried out several tests for positron-He collisions. We first tried many different (Cartesian Gaussian) basis sets in a single-excitation configuration-interaction (CI) framework. Then, we included single- and double-excitations of the target in the CI expansion (CISD) of the scattering wave function. Finally, we tried to mimic the virtual positronium cusp. It seems that cusp description should indeed be further improved. (C) 2002 Elsevier Science B.V. All rights reserved.

Nuclear Instruments & Methods in Physics Research Section B- Beam Interactions with Materials and Atoms 192[1-2], 225-237. 2002.

P 085 - 02 "Uncertainty relations for entangled states".

Rigolin, G.

A generalized uncertainty relation for an entangled pair of particles is obtained if we impose a symmetrization rule for all operators that we should employ when doing any calculation using the entangled wave function of the pair. This new relation reduces to Heisenberg's uncertainty relation when the particles have no correlation and suggests that we can have new lower bounds for the product of position and momentum dispersions.

Foundations of Physics Letters 15[3], 293-298. 2002.

Abstracta

Instituto de Física

Diretor: Prof. Dr. Daniel Pereira

Universidade Estadual de Campinas - UNICAMP

Cidade Universitária C.P. 6165

CEP: 13081-970 - Campinas - SP - Brasil

e-mail: secdir@ifi.unicamp.br

Fone: 0XX 19 3788-5300 / Fax: 0XX 19 3788-3127

Publicação

Biblioteca do Instituto de Física Gleb Wataghin

<http://www.ifi.unicamp.br/bif>

Diretora Técnica: Rita Aparecida Sponchiado

Elaboração

Tânia Macedo Folegatti

abstract@ifi.unicamp.br

Projeto Gráfico

ÍgneaDesign

Impressão

Gráfica Central - Unicamp

